Thermal Fronts Generated by Internal Waves Propagating Obliquely along the Continental Slope*

Johannes R. Gemmrich and Hans van Haren

Netherlands Institute for Sea Research, Texel, Netherlands

(Manuscript received 28 April 1999, in final form 27 April 2000)

ABSTRACT

Rapid temperature falls occurring at semidiurnal periods are observed close to the bottom above the continental slope in the Bay of Biscay. Simultaneous current measurements reveal that the abrupt temperature decrease $O(0.5 \text{ K})$ within one minute is associated with a brief downslope current, contrary to previous observations. It is suggested that the flow field associated with internal waves propagating obliquely downslope is responsible for advecting denser water higher on the slope than lighter fluid, resulting in a gravitationally unstable stratification. The collapse of this stratification is observed as a thermal front passing the moored instruments.

1. Introduction

Interactions of internal waves and sloping boundaries can lead to turbulent boundary mixing (Eriksen 1985; Ivey and Nokes 1989; De Silva et al. 1998) and may play an important role in diapycnal diffusion in the deep ocean (Munk 1966; Armi 1978; Munk and Wunsch 1998). Studies of wave–boundary interactions are mainly focusing on processes associated with reflection of internal waves and are often restricted to the case of wave propagation in a plane normal to the sloping boundary. Internal waves reflecting from a sloping boundary preserve their frequency and an incident wave preserves its angle to the vertical upon reflection rather than normal to the boundary. Near critical conditions, when the boundary slope matches the inclination of the group velocity vector of the reflected wave, wave breaking may occur. Furthermore, the locked phase relationship between incident and reflected waves allows for continuous nonlinear interactions that can generate thermal fronts (Thorpe 1992). However, the geometry of critical wave reflection, where the incident wave propagates its energy downward from the interior toward the sloping bottom, is rather specific. Especially, internal tides generated at the continental shelf edge are generally not reflected at the continental slope but propagate away from the slope (Pingree and New 1989).

Incident waves traveling obliquely to the slope are associated with significant instantaneous alongslope currents and generate a mean alongslope flow (Thorpe 1997; Dunkerton et al. 1998) that is typically $O(0.01 \text{ m s}^{-1})$ and somewhat larger if breaking occurs (Thorpe 1999a). Fronts may form for a wide range of angles of incidence by steepening of isopycnal surfaces induced by the instantaneous upslope flow (Thorpe 1999b; Thorpe and Lemmin 1999).

Here we present observations of near-bottom thermal fronts occurring at semidiurnal (M_2) frequency above the continental slope in the Bay of Biscay. Similar fronts have been observed previously at various locations on the continental slope (Thorpe 1987; White 1994) and these fronts are thought to be caused by internal tides reflecting from the slope (Thorpe 1992). However, our observations are not consistent with the properties of reflected internal waves. Instead, we propose that an upslope advection of denser fluid associated with internal waves propagating obliquely downslope may generate a gravitationally unstable stratification. The collapse of this stratification results in an abrupt temperature decrease combined with a downslope flow. A very drastic example of such a collapse has been observed by a U.S. Navy minisub on a sloping site in the Faeroe–Shetland channel (cited in Sherwin 1991). They report "swirls of sand and dust," which occurred regularly at the semidiurnal tidal period combined with a sharp temperature drop and a rapid increase of alongslope velocity.

2. Observations

Continuous measurements of temperature and velocity structure were obtained for a period of 22 days in

---

* Netherland Institute for Sea Research Contribution Number 3381.

Corresponding author address: Dr. Johannes Gemmrich, NIOZ, P.O. Box 59, 1790 AB Den Burg, Texel, Netherlands.
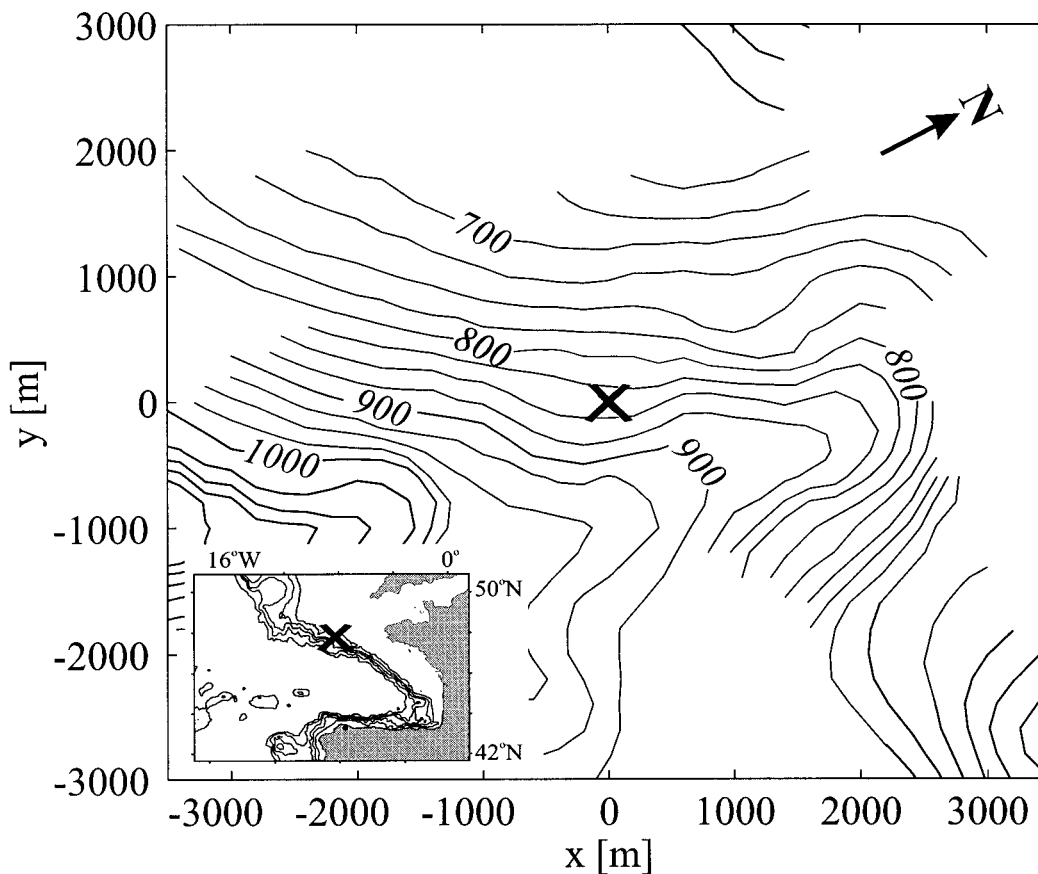E-mail: gemmrich@nioz.nl

Fig. 1. Bathymetry of the deployment site in a slope-oriented coordinate system (isobaths in meters), based on ~1800 echo soundings within ±10 km of the deployment site. The cross indicates position of the bottom-lander. Insert: Deployment site in Bay of Biscay. Isobaths shown are 200 m, 1000 m, 2000 m, 3000 m and 4000 m.

the near-bottom layer above the continental slope in the Bay of Biscay at 48°03.8′N, 8°19.9′W. Two acoustic Doppler current profilers (ADCPs), mounted rigidly on a bottom lander, were combined with a thermistor string, which provided temperature profiles between 2.9 and 33.9 m above the bottom. The upward-looking 600 kHz ADCP rendered velocities between 4.9 and 47.9 m above the bottom at 1-m intervals (bins). Spatial resolution of 1 m was also achieved for the temperature measurements. Swaying of the thermistor string, monitored with a tilt meter at the top of the string, was <12°, resulting in a maximum vertical displacement of the top sensor <0.75 m. A second, downward-looking 1200-kHz ADCP, placed ~2.5 m to the side of the 600 kHz ADCP, resolved velocities at 1.04–2.04 m above the bottom in 0.25-m intervals. Standard deviation of the horizontal velocities are 8.6×10^{-3} m s^{-1} for the 600-kHz ADCP and 7.6×10^{-3} m s^{-1} for the 1200-kHz ADCP. Standard deviations of the vertical components are about four times smaller. Sampling rate for all sensors was once per 30 seconds so that the buoyancy frequency $N = 2.0 \pm 0.7 \times 10^{-3}$ s^{-1}, estimated from two CTD profiles, is well resolved. The local inertial

frequency at the deployment location is $f = 1.085 \times 10^{-4}$ s^{-1}.

The instrumentation had been deployed on the shoreward side of a large trench at water depth of 820 m (Fig. 1). However, within the tidal excursion in along-isobath direction the bathymetry is relatively smooth and the slope orientation is well defined. The slope angle depends on the considered horizontal scale, which is determined by the relevant physical processes. For studies on internal wave reflection, we adopt the projection of the wave beamwidth, which is monitored by the vertical profiling range as an appropriate horizontal scale. An upper limit for this scale is given by the cross-isobath distance at which a depth difference equal to the ADCP profiling range is achieved. In our case, this distance is $O(500$ m), yielding a mean bottom slope $\alpha = 4.9°$ around the mooring. However, for a cross-slope scale of 1000 m the estimated bottom slope increases to $\alpha_{1000} = 5.2°$, whereas for smaller scales the slope estimate slightly decreases. The mean bottom slope $\alpha = 4.9°$ is larger than the critical slope for semidiurnal internal tides $\alpha_{M_2\mathrm{cr}} = 2.9° \pm 1°$ but less than the critical slope for the M_4 component $\alpha_{M_4\mathrm{cr}} = 8.5° \pm 3°$. The uncer-

tainties are based on the bounds of the buoyancy frequency. The critical wave frequency is $\sigma_{cr} = 2.8 \pm 0.7$ cpd. In the following, an orthogonal, bottom-oriented coordinate system is adopted with the x direction being aligned with the isobaths (alongslope), the y direction being cross-isobath and positive toward shallower water (cross-slope), and the z axis is bottom-normal and positive upward. The velocities, originally recorded in an earth-referenced coordinate system, have been converted accordingly.

At all depths within the measurement range temperature and velocity fields are dominated by M_2 fluctuations. The cross-slope velocity component v exhibits a similarly large M_4 component. The current is mainly directed in an alongslope direction. Maximum values of alongslope, cross-slope, and bottom-normal current components are $u = \pm 0.6$ m s^{-1}, $v = \pm 0.25$ m s^{-1}, $w = \pm 0.06$ m s^{-1}, respectively. Associated with these currents are temperature fluctuations of up to 2 K within one tidal period (Fig. 2). Throughout the monitored range the mean current, averaged over the complete deployment period, is oriented in downslope and negative alongslope direction. Near the bottom the mean current magnitude increases slightly from 7×10^{-2} m s^{-1} to a maximum of 9×10^{-2} m s^{-1} at 5 m above the bottom. Above that height it decreases monotonically to 2×10^{-2} m s^{-1} at the top of the profile. The mean bottom-normal velocity is negative at all depths with a maximum of -3×10^{-3} m s^{-1} at 5 m. At our lowest measurement bin, 1 m above the bottom, $|\overline{w}| < 10^{-3}$ m s^{-1}. This supports the estimate of the bottom slope. Mean temperature gradients calculated for the complete deployment period are 12×10^{-3} km^{-1} between 2.9 m and 14.9 m and 7×10^{-3} km^{-1} in the layer 14.9–33.9 m, implying a strong mean near-bottom stratification. A more detailed description of the current and temperature field is given in Gemmrich and van Haren (2000, manuscript submitted to *J. Mar. Res.*).

A striking feature of this dataset is the abrupt temperature changes of up to 0.7 K within one minute (Fig. 3), representing the passage of a thermal front. This event occurs every tidal cycle, although not always as pronounced. During neap tide the magnitude of the temperature fall is smaller (~0.4 K) and more spread out in time than during spring tide. Generally, the thermal front passes the sensors within 5–15 min minutes after the reversal from negative to positive alongslope flow occurs (Fig. 4). A time delay of 2–3 samples between the onset of the signal at the lowest thermistor and the uppermost sensor cannot be explained by the swaying of the thermistor string but indicates a vertical inclination of the front. Associated with the temperature fall is a reversal of the cross-slope current from upslope to downslope and a sudden increase of the alongslope current speed by up to 0.3 m s^{-1}.

3. Discussion

The reversal of the alongslope current just a few minutes prior to the frontal passage excludes mean flow advection of alongslope temperature gradients as the origin of the observed temperature change. Previous observations of these rapid changes in density have been attributed to nonlinear features of internal wave reflection (Thorpe 1992, 1999b). This mechanism predicts rapid density changes, associated with cold water moving upslope, occurring once per tidal cycle at the time of maximum flow. However, in our observations thermal fronts are associated with cold water moving downslope and they occur within a few minutes (1/50 of the wave period) after the reversal of the alongslope current (Fig. 4). Hence, the observed thermal fronts are not consistent with nonlinear resonance of internal wave reflection as a generation mechanism.

Bandpass (1.5–2.5 cpd) filtered velocity and temperature records indicate an upward phase propagation, that is, downward energy propagation at the M_2 period. There are two possible configurations leading to the described wave propagation properties. First, an internal tide is generated at the shelf break and is propagating downslope and, second, an internal tide propagating downward from an offshore direction is being reflected farther upslope of the deployment site and the reflected and amplified beam is being observed. At a single location both scenarios yield similar near-bottom currents and temperature perturbations and cannot be distinguished unambiguously from our dataset. However, in both cases the downward propagating wave dominates the current signal and the major axis of the current ellipse within the specified frequency band defines the orientation θ of the bottom projection of the internal tide propagation (Fig. 5b). This angle varies between $-5°$ and $25°$ with a mean value $\theta \sim 10°$. Hence, the properties of the currents at the M_2 period suggest the presence of an internal tide oriented obliquely to the main slope and with energy propagating from the shelf break toward the abyssal plane.

In the undisturbed case, isotherms are parallel to isobaths with lower temperatures downslope. Internal waves that are not aligned with the mean slope may tilt these isotherms by advecting colder water upslope and warmer water downslope. The strength of the advection increases with the wave amplitude. Depending on the phase of the wave (Figs. 5b,e) this process creates once per wave period a gravitationally unstable stratification (Fig. 6). The collapse of this instability results in a rapid temperature change similar to what is observed.

Two unique features of obliquely incident internal waves on a sloping bottom are mainly responsible for the front generation. First, the effective bottom slope along the ray path $\alpha_{eff} = \sin^{-1}(\sin\alpha \, \sin\theta)$ is less than the slope α perpendicular to the isobaths. The bottom slope at the measurement site is steeper than the inclination β of the group velocity vector of internal semidiurnal tides and only higher frequency waves or internal semidiurnal tides originating in the ocean basin could reach the bottom. However, in the configuration described above even the maximum effective bottom
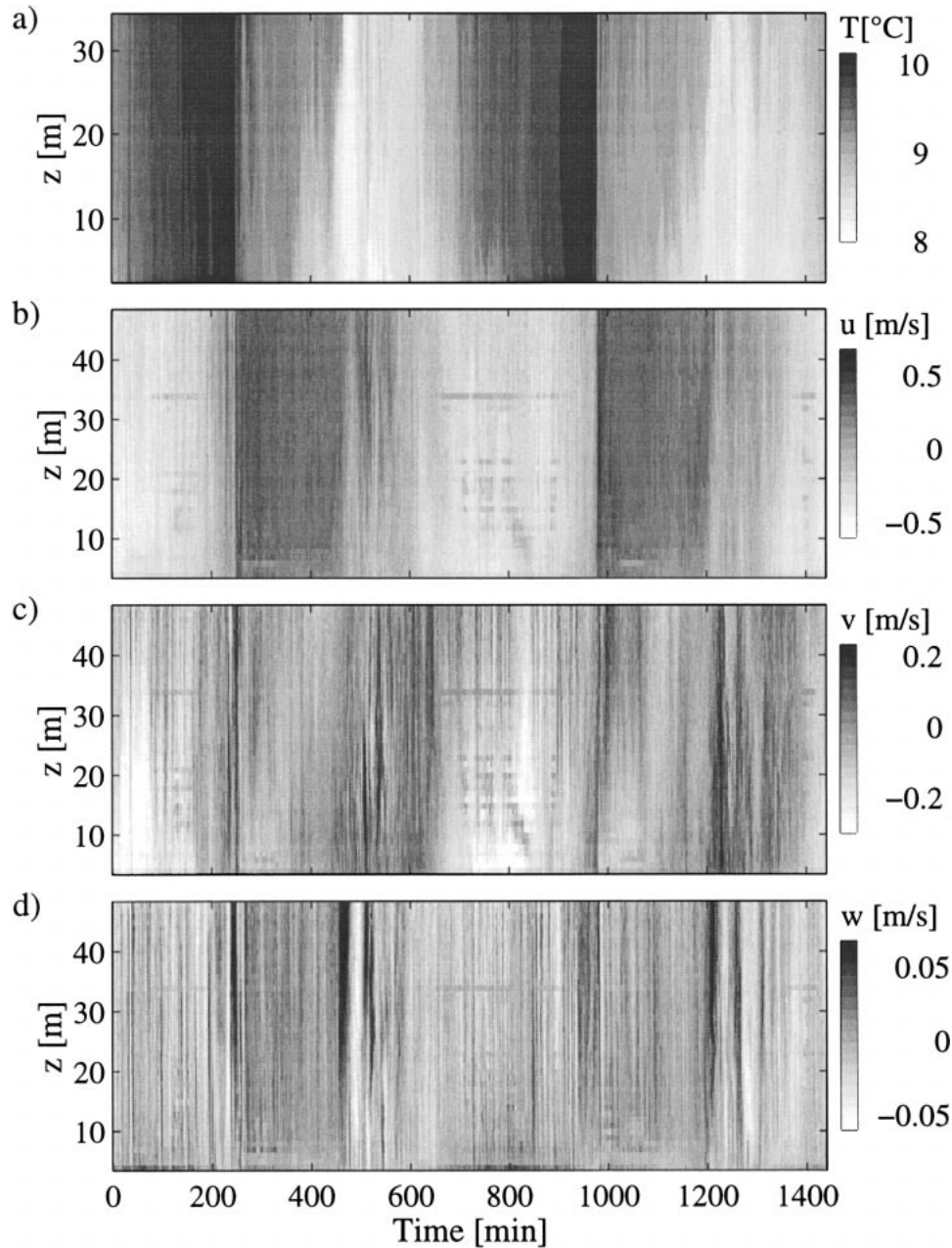
FIG. 2. Temperature and velocity field for two tidal cycles during spring tide: (a) temperature T assuming nominal thermistor height, (b) alongslope velocity u, (c) cross-slope velocity v, and (d) bottom-normal velocity w. The banding of velocities at ~10 m to 25 m and at 34 m occurring during negative alongslope currents are caused by interference of the thermistor string with one of the acoustic beams and do not represent correct current fluctuations.

slope allows downward-propagating internal semidiurnal tides to interact with the bottom, that is, $\alpha_{\mathrm{eff}} < \beta$. Second, the intersection line of a surface of constant wave phase with the sloping bottom is neither parallel nor perpendicular to the isobaths. The obliqueness of this line of intersection, specified by the angle φ, is essential for the assumed instability mechanism. The intersection lines of different constant phase surfaces are parallel but displaced along the ray path (Fig. 5a). Thus, depending on the phase of the internal tide, divergence or convergence are generated along a line inclined by φ. This flow pattern is associated with upslope advection of colder water and downslope advection of warmer water (Fig. 2). [Note, this process of front generation occurs prior to the frontal passage, where cold water is associated with a brief downslope current (Fig.
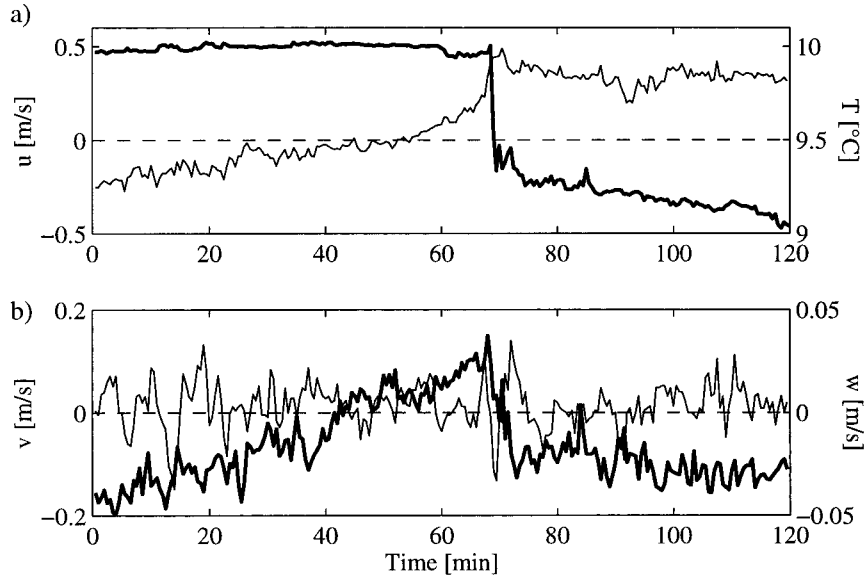
FIG. 3. Velocity and temperature at 7.9 m above the bottom showing passage of a thermal front: (a) temperature (thick line) and alongslope current component (thin line) and (b) cross-slope (thick line) and bottom-normal current component (thin line). Time interval shown corresponds to $t = 910$ min to $t = 1030$ min in Fig. 2.

3).] Convergences generate fronts with cold water on the upslope side of the front and warm water below, the velocity field leading the temperature field. At M_2, the phase between current and temperature is 100° for the alongslope velocity component and 140° for the cross-slope component. Hence, the strongest cross-slope temperature gradient occurs close to the time of reversal

from convergence to divergence, which for $0° < \theta < 90°$, coincides with the flow reversal from negative to positive along-slope current (Fig. 6). The magnitude of the cross-slope temperature gradient is a function of the wave amplitude as well as the front inclination φ. If the gradient is large enough for the buoyancy force to overcome bottom friction, cold dense water flows down-
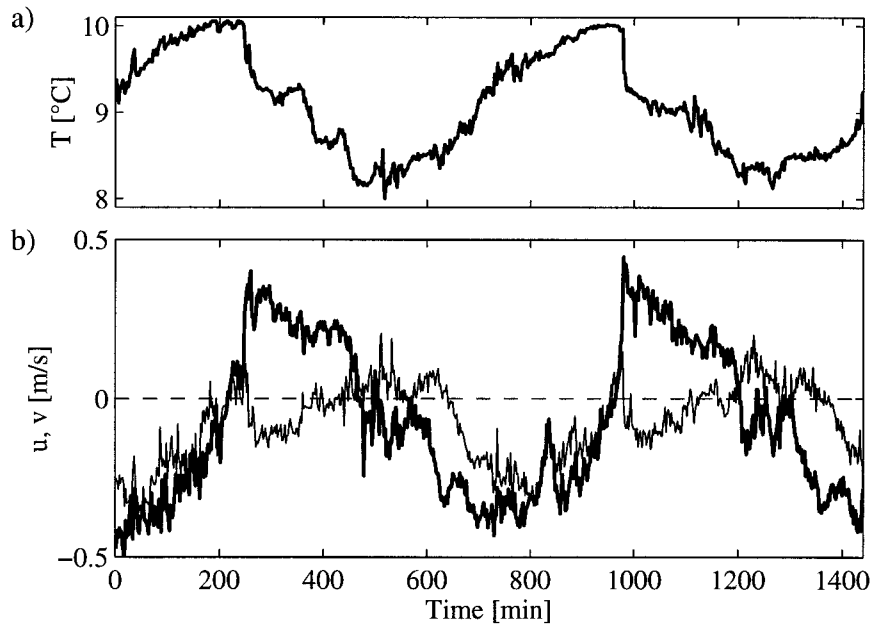

FIG. 4. Temperature and velocity at 7.9 m above the bottom illustrating occurrence of thermal front passages: (a) temperature and (b) alongslope (thick line) and cross-slope current component (thin line). Same time interval shown as in Fig. 2.
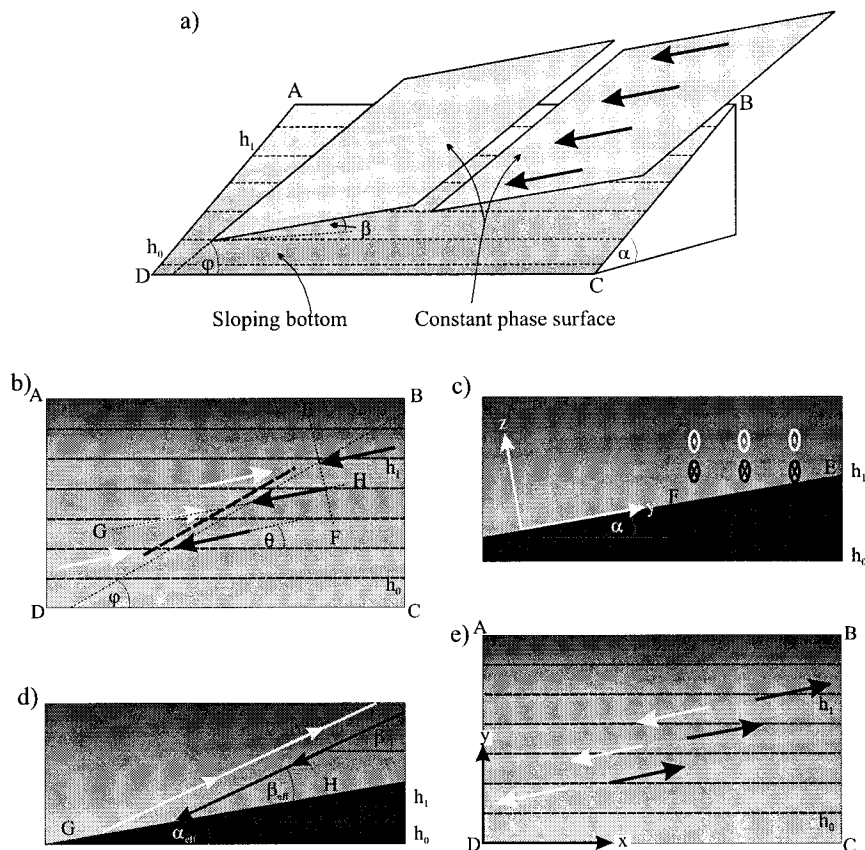
FIG. 5. Sketch defining the notation and showing the wave particle motion (thick arrows) associated with internal tides propagating obliquely to a slope. For clarity only a narrow beam containing one wavelength is shown. The anticipated wave is periodic in space. (a) Constant phase surfaces intersecting with the sloping boundary. Thin dashed lines indicate isobaths with h_0 deeper than h_1, and undisturbed isotherms with colder water at h_0. (b) Plan view of the sloping bottom at $t = t_0$. The thick dashed line depicts convergence line where a thermal front is being generated; thin dashed lines as in a. Arrows represent the bottom projection of the wave particle motion. (c) Side view at $t = t_0$ along a line EF perpendicular to the group velocity vector, (d) side view at $t = t_0$ along a line GH parallel to the group velocity vector, (e) same as b but at $t = t_0 + \tau/2$, where τ is the wave period.

slope. This collapse of the front causes a rapid temperature decrease associated with downslope flow, similar to what we observe. Furthermore, for $0° < \theta < 90°$ a temperature decrease is linked to positive alongslope currents, whereas during periods of negative alongslope currents temperature increases. This is entirely consistent with our observations (Fig. 2).

Generally, oblique internal waves on a sloping boundary may create lines of convergence and divergence at the boundary. In the presence of cross-slope temperature gradients this leads to the generation of thermal fronts. However, the existence of thermal fronts and their orientation on the slope depend on four parameters: the boundary slope α, the angle β between the group velocity vector and the horizontal plane, the angle θ between isobaths and boundary projection of the group velocity vector, as well as the wave amplitude. From a geometrical derivation the orientation of the front, φ, follows as

$$\varphi = \theta + \sin^{-1}\left[\frac{\sin\gamma}{\left(1 + \dfrac{\tan^2\alpha}{\sin^2\beta_{\text{eff}}} + 2\dfrac{\tan\alpha \, \cos\gamma}{\sin\beta_{\text{eff}}}\right)^{1/2}}\right], \quad (1)$$

where $\gamma = \theta + 90°$ and the effective inclination of the group velocity vector $\beta_{\text{eff}} = \beta - \alpha_{\text{eff}}$ is defined as the angle between the group velocity and its boundary projection (Fig. 5). For conditions typical in this dataset ($\alpha = 4.9°$, $\beta = 2.7°$, $\theta = 10°$) the predicted front angle is $\varphi = O(30°)$ and favorable for generating thermal fronts.

An earlier experiment took place farther southeast where the bottom slope is $a \approx 15.7°$. During that experiment the buoyancy frequency was similar to that at our site. Hence, for internal tides to reach the bottom, that is, $\beta_{\text{eff}} > 0$, and, therefore, to be able to generate boundary convergences the waves would have to propagate nearly parallel to the slope ($\theta < 8°$), yielding a front orientation angle $\varphi < 10°$. No thermal fronts are
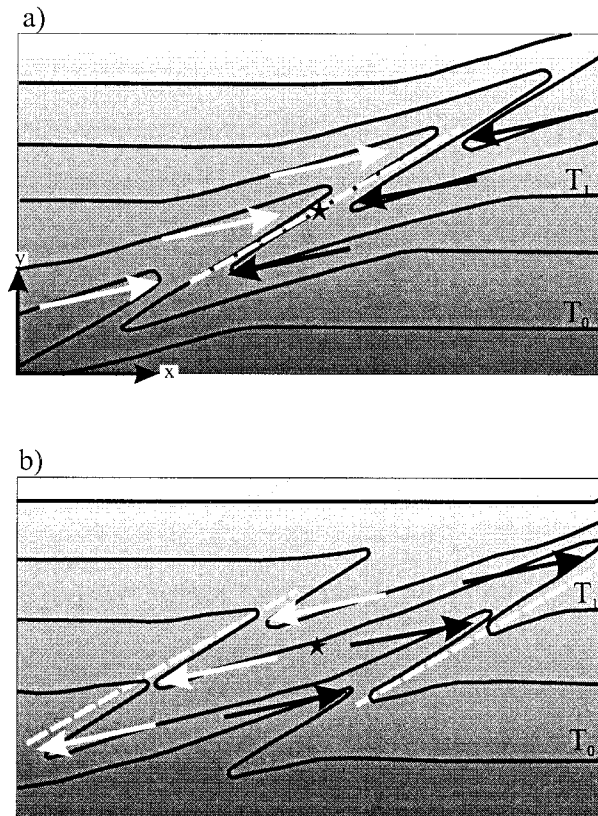
FIG. 6. Plan view (Figs. 5b,e) of idealized distortion of initially parallel isotherms due to cross-slope temperature gradients being advected by oblique internal waves. Note that for clarity the flow field (arrows) presents conditions at a quarter wave period prior to the instant of the depicted temperature field. Only a narrow beam, containing one wavelength of a periodic wave, is shown. Dashed lines mark location where a thermal front is being generated. Here $T_0 < T_1$. The star represents the measurement site: (a) $t = t_0$, representing unstable stratification at measurement site, (b) $t = t_0 + \tau/2$, representing stable stratification at measurement site.

observed at that site, although the magnitude of the current was comparable to the conditions described here. It is likely, that the potential cross-slope temperature gradient associated with the weak cross-slope advection and the front angle are too small to generate the proposed instability.

However, for more gentle slopes of $O(5°)$ and typical buoyancy frequencies $O(2 \times 10^{-3} \text{ s}^{-1})$ interactions between internal tides, which propagate downward and in offshore direction, and the bottom are possible for a wide range of propagation azimuths ($|\theta| < 40°$) and are independent of the exact position on the slope. Hence, thermal fronts associated with such a configuration of internal tide propagation and bottom slope can be expected frequently in the near-bottom layer of continental slopes. Recent observations on a gentle slope of the Faeroe–Shetland channel reveal abrupt temperature decreases as dramatic as the observations described here (H. van Haren, unpublished results). The bottom to-

pography at the Faeroe–Shetland site is rather smooth, supporting our interpretation that the observations described here are not primarily governed by the presence of irregular features of the slope. We anticipate that, despite the brief duration of the event, the collapse of the thermal fronts and the associated current fluctuations represent a significant contribution to the average heat and momentum fluxes supported within the internal wave band.

REFERENCES

Armi, L., 1978: Some evidence for boundary mixing in the deep ocean. *J. Geophys. Res.,* **83,** 1971–1979.
De Silva, I. P. D., J. Imberger, and G. N. Ivey, 1998: Breaking of super-critically incident internal waves at a sloping bed. *Physical Processes in Lakes and Oceans,* No. 54, Coastal and Estuarine Studies, Amer. Geophys. Union, 475–484.
Dunkerton, T. J., D. P. Delisi, and M.-P. Lelong, 1998: Alongslope current generated by obliquely incident internal gravity waves. *Geophys. Res. Lett.,* **25,** 3871–3874.
Eriksen, C. C., 1985: Implications of ocean bottom reflection for internal wave spectra and mixing. *J. Phys. Oceanogr.,* **15,** 1145–1156.
Ivey, G. N., and R. I. Nokes, 1989: Vertical mixing due to the breaking of critical internal waves on sloping boundaries. *J. Fluid Mech.,* **204,** 479–500.
Munk, W. H., 1966: Abyssal recipes. *Deep-Sea Res.,* **13,** 207–230.
——, and C. Wunsch, 1998: Abyssal recipes II: Energetics of tidal and wind mixing. *Deep-Sea Res. I,* **45,** 1977–2010.
Pingree, R. D., and A. I. New, 1989: Downward propagation of internal tidal energy into the Bay of Biscay. *Deep-Sea Res.,* **36,** 735–758.
Sherwin, T. J., 1991: Evidence of a deep internal tide in the Faeroe–Shetland channel. *Tidal Hydrodynamics,* B. B. Parker, Ed., Wiley and Sons, 469–488.
Thorpe, S. A., 1987: Currents and temperature variability on the continental slope. *Philos. Trans. Roy. Soc. London,* **323A,** 471–517.
——, 1992: Thermal fronts caused by internal gravity waves reflecting from a slope. *J. Phys. Oceanogr.,* **22,** 105–108.
——, 1997: On the interactions of internal waves reflecting from slopes. *J. Phys. Oceanogr.,* **27,** 2072–2078.
——, 1999a: The generation of along-slope currents by breaking internal waves. *J. Phys. Oceanogr.,* **29,** 29–38.
——, 1999b: Fronts formed by obliquely reflecting internal gravity waves at a sloping bottom. *J. Phys. Oceanogr.,* **29,** 2462–2467.
——, and U. Lemmin, 1999: Internal waves and temperature fronts on slopes. *Ann. Geophys.,* **17,** 1227–1234.
White, M., 1994: Tidal and subtidal variability in the sloping benthic boundary layer. *J. Geophys. Res.,* **99,** 7851–7864.